

by the following mechanism: the intermediate acetyl chloride was enolized firstly, and then added with chlorine to produce the chloroacetyl, which did rapid chlorine exchange reaction with acetic acid to generate the monochloroacetic acid and acetyl chloride.

Y. Ogata and T. Sugimoto *et al*⁵ investigated the ionic mechanism of the synthesis of monochloroacetic acid. Y. Ogata and T. Harada *et al*⁶ indicated that di- and trichloroacetic acids were generated by ionic chlorination in the synthesis process of monochloroacetic acid. Y. Ogata *et al*⁶ also found that the chloroacetyl chloride could be produced by enolization of acetic acid by acid catalysis added with chlorine. T. Salmi *et al*⁷ proposed that the rate-determining step of the chlorination of acetic acid was the acid-catalyzed enolization of acetyl chloride. P. Maki-Arvela and T. Salmi⁸ found that acetyl chloride could be formed *in situ* in the chlorination process by allowing acetic anhydride to react with HCl, and they proposed the acid-catalyzed autocatalysis effect. X. Y. Zhou⁹ also believed that chlorination of monochloroacetic and dichloroacetic acids was the ionic mechanism, and belonged to the consecutive reactions. P. Maki-Arvela *et al*¹⁰ indicated that the generation of dichloroacetic acid had two routes: the ionic mechanisms and the radical mechanisms.

In order to verify the synthesis mechanism of monochloroacetic, di- and trichloroacetic acids, the Dmol3 program of Materials Studio 5.5 was applied to simulate the mechanism of chlorination of acetic acid using the density function method. The results could contribute to promote the production of monochloroacetic acid.

EXPERIMENTAL AND CALCULATION

Experimental

The chlorination of acetic acid was carried out in a homemade glass tube equipped with a magnetic stirring apparatus. The glass tube was heated by an oil bath heater with a temperature controller. The chlorine gas was metered by a rotameter to disperse into the reaction mixture. A reflux

condenser equipped with low temperature cooling circulating pump was placed on the top of the reactor. The gaseous compounds passed through water, sodium bicarbonate solution and concentrated sodium hydroxide solution before being released to the air.

The acetic acid to be chlorinated was placed in the reaction vessel. The slightly excess chlorine feed was introduced, and the liquid phase was heated to the desired reaction temperature. A certain amount of acetic anhydride was added. Samples of the liquid phase were analyzed by gas chromatograph after esterification.¹¹

Calculation Methods

Density functional theory method quantum chemistry calculation was adopted and the calculations were performed by using the Dmol³ program mounted on Materials Studio 5.5 package. All the reactions and products in the chlorination reaction were optimized and their stable structures were obtained at the same time. All transition states of the reactions were trialed and searched carefully by using an LST/QST method, thus, the primitive activation energy and the heat of reaction were obtained. The nonlocal exchange and correlation energies were calculated with the PW91 function of the generalized gradient approximation (GGA)¹¹ and a double numerical plus polarization (DNP) basis set in the level of all electrons. The convergence criteria included threshold values of 1×10^{-5} Hartree, 0.02 Hartree per nm, and 0.0005 nm for energy, force and displacement convergence, respectively, the self-consistent-filled (SCF) density convergence threshold value was specified as 1×10^{-6} Hartree. A Fermi smearing of 0.005 Hartree was employed to improve the computational performance, and the solvent effect was also considered during the calculations. The geometries of all stationary points were optimized at this level.

RESULTS AND DISCUSSION

The experimental results

The effect of different catalyst amounts of acetic anhydride in chlorination: First, the effect of acetic acid catalytic chlorine was investigated (see Table 1 and Figure 1) in the condition of 105°C reaction temperature, 40mL/mins chlorine flow rate and acetic anhydride were 8%; 15%; 20% and 25% of the quality of acetic acid.

Table 1

The catalyst amount of acetic anhydride in chlorination

Acetic anhydride (%)	Reaction time (h)	CA (%)	MCA (%)	DCA (%)
8	6	73.37	23.51	3.12
15	6	51.72	45.04	3.24
20	6	21.29	76.41	2.30
25	6	9.53	88.39	2.08

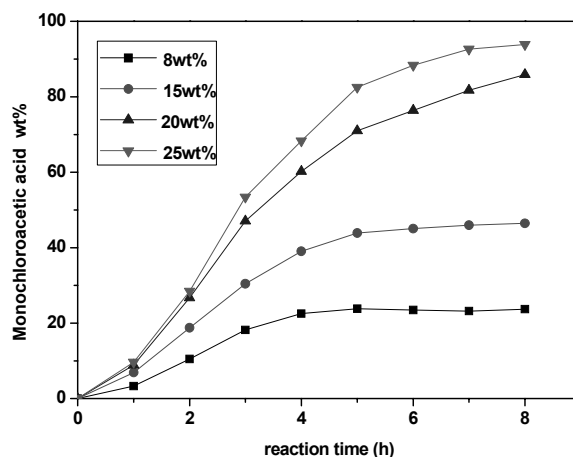


Fig. 1 – The effect of catalyst amount of acetic anhydride on monochloroacetic acid generation.

As shown in Figure 1, the production amount of monochloroacetic acid increased with time after the addition of acetic anhydride. The generation rate of monochloroacetic acid was slow in the first 1h and increased remarkably until 6h, then, its generation rate increased steadily from 6h to 8h. At the same time, the rate and productions of monochloroacetic acid also increased rapidly with the increase of acetic anhydride mass fraction. Moreover, we found that the productions of dichloroacetic acid decrease with the increasing of acetic anhydride mass in Table 1.

The influence of concentrated H_2SO_4 and $FeCl_3$ catalyst promoter in chlorination: In order to verify the catalytic principle, 1.5% $FeCl_3$ and 5% concentrated H_2SO_4 were added in the experiment of acetic anhydride catalytic chlorination. The comparison of the chlorination reaction and the blank experiment indicated the catalytic effect of acid and autocatalytic of the reaction. Chloride products were analyzed by gas chromatography (see Figure 2 and Table 2).

As was shown in Figure 2 and Table 2. The generation rate of monochloroacetic acid was very fast in the first 50 mins with the addition of concentrated H_2SO_4 or $FeCl_3$, and the yield of monochloroacetic acid was 30% and 20% respectively, however, the yield of monochloroacetic acid was only 4% in the blank experiment. Then, the generation of monochloroacetic acid increased rapidly from 50 mins to 150 mins, the yield was 97.6% and 91.7%, respectively. And the yield of monochloroacetic acid was 29.5% in the blank experiment. Moreover, the yield of monochloroacetic acid began to decrease to 94.2% with the increase of concentrated H_2SO_4 catalyst promoter, but the yield of monochloroacetic acid kept on increase with $FeCl_3$ catalyst promoter and reached 95.8% during 150 mins to 200 mins. Then, when the reaction time reached 150mins, the yield of dichloroacetic acid was 0.74%, the yield of dichloroacetic acid was 2.01% and 2.79% with the concentrated H_2SO_4 and $FeCl_3$ catalyst promoter, respectively, which was higher than the yield of dichloroacetic acid in the blank experiment.

Table 2

The influence of catalyst promoter on monochloroacetic acid

Catalyst promoter	Mass (%)	Reaction time (min)	CA (%)	MCA (%)	DCA (%)
blank	0	150	69.9	29.5	0.74
H_2SO_4	5	150	0.44	97.6	2.01
$FeCl_3$	1.5	150	0.09	91.7	2.79

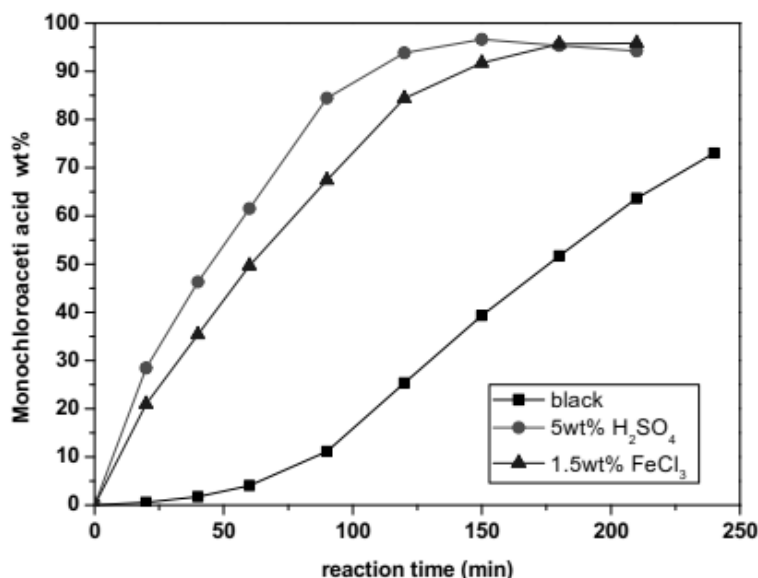
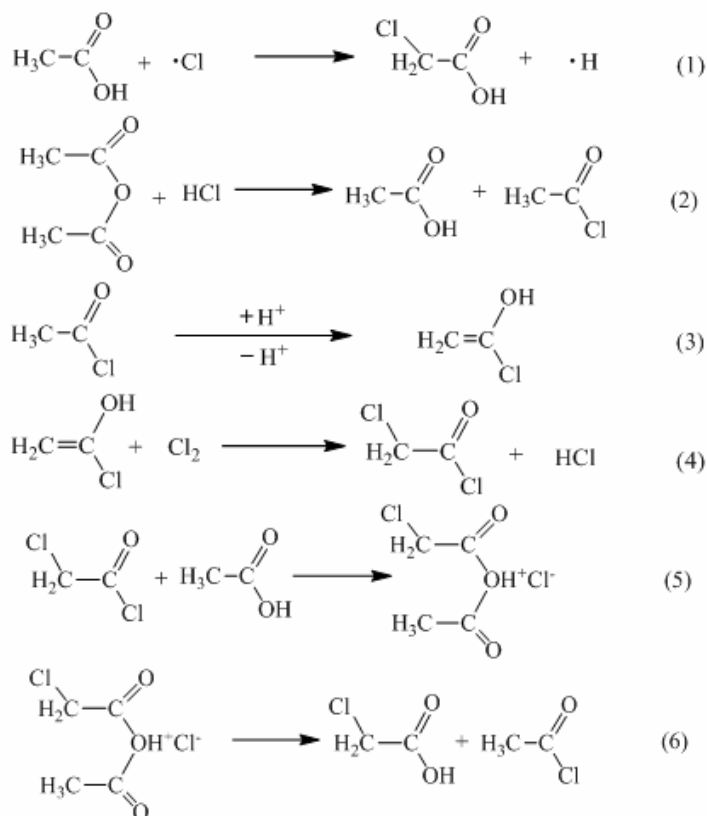


Fig. 2 – The influence of catalyst promoter in chlorination.

Synthesis mechanism of monochloroacetic acid

In order to investigate the formation route of monochloroacetic acid, two possible reaction paths were constructed: the radical chlorination mechanism and the ionic chlorination mechanism

(Scheme 1). The path 1 was the formation route of monochloroacetic acid *via* radical chlorination mechanism [Scheme 1, Equation (1)]. The path 2 was the formation route of monochloroacetic acid *via* ionic chlorination mechanism [Scheme 1, Equation (2)-(6)].



Scheme 1 – Path of monochloroacetic acid generation.

The configurations of reactants and products were built and the geometry structure was optimized. Transition states were investigated based on the calculation of the basis reactants and products. Each reaction transition state was derived from the potential energy surface at the highest point of the potential energy corresponding to the configuration. Frequency analysis showed that these configurations were the only virtual frequency. Energy of reactants, products and transition states to relevant primitives and the corresponding virtual frequency of the transition state were presented in Table 3. At the same time, energy potential diagram of the primitive reactions with corresponding reactions, transition states and products of configuration were shown in Figure 3.

The results showed that the route of monochloroacetic acid formation *via* ionic chlorination mechanism was as follows. First, acetic anhydride conducted initially [Scheme 1, Equation (2)] and formed acetyl chloride. Its reaction activation energy was 5.23kJ/mol. Then,

acetyl chloride conducted the enolization [Scheme 1, Equation (3)] and formed 1-chloro, 1-ethene-1-ol and the corresponding primitive activation energy was 51.64 kJ/mol. Since then, the double bond in 1-chloro, 1-ethene-1-ol was apt to react with chlorine [Scheme 1, Equation (4)] and formed chloroacetyl chloride, and the corresponding primitive activation energy was 30.04kJ/mol. Finally, the -OH and -Cl exchange reaction generated monochloroacetic acid [Scheme 1, Equation (5) and (6)] and their activation energy was 15.42kJ/mol and 0.75kJ/mol, respectively. Therefore, reaction (2) was the catalyst initiation reaction among the whole reactions from (2) to (6) and the acetic anhydride reaction formed a real catalyst, namely, acetyl chloride. The whole reaction process became acid catalytic reaction once acetyl chloride was formed. More importantly, the acidity of monochloroacetic acid was stronger than the acetic acid, so the acid catalytic reaction was accelerated.

Table 3

Possible elementary reactions involved in monochloroacetic acid and byproducts synthesis together with the activation energies (Ea) and reaction energies (ΔH)

Step	Chemical reaction	Frequency (cm^{-1})	Ea ($\text{kJ}\cdot\text{mol}^{-1}$)	ΔH ($\text{kJ}\cdot\text{mol}^{-1}$)
(1)	$\text{CH}_3\text{COOH}+\cdot\text{Cl}\rightarrow\cdot\text{H}+\text{C}_2\text{H}_3\text{O}_2\text{Cl}$	-318.33	162.45	136.07
(2)	$(\text{CH}_3\text{CO})_2\text{O}+\text{HCl}\rightarrow\text{CH}_3\text{COOH}+\text{CH}_3\text{COCl}$	-75.98	5.23	-33.41
(3)	$\text{CH}_3\text{COCl}+\text{H}^+\rightarrow\text{H}^++\text{C}_2\text{H}_2\text{ClOH}$	-1406.50	51.64	-84.73
(4)	$\text{C}_2\text{H}_2\text{ClOH}+\text{Cl}_2\rightarrow\text{HCl}+\text{CH}_2\text{ClCOCl}$	-38.43	30.04	-138.89
(5)	$\text{CH}_2\text{ClCOCl}+\text{CH}_3\text{COOH}\rightarrow\text{C}_4\text{H}_6\text{O}_3\text{Cl}_2$	-69.47	15.42	6.21
(6)	$\text{C}_4\text{H}_6\text{O}_3\text{Cl}_2\rightarrow\text{C}_2\text{H}_3\text{OCl}+\text{CH}_2\text{ClCOOH}$	-49.31	0.75	-4.41
(7)	$\text{CH}_3\text{COOH}+2\cdot\text{Cl}\rightarrow 2\cdot\text{H}+\text{CHCl}_2\text{COOH}$	-271.91	186.37	158.84
(8)	$\text{CH}_2\text{ClCOOH}+\cdot\text{Cl}\rightarrow\cdot\text{H}+\text{CHCl}_2\text{COOH}$	-115.62	168.75	136.31
(9)	$\text{CH}_2\text{ClCOCl}+\text{H}^+\rightarrow\text{H}^++\text{C}_2\text{HCl}_2\text{OH}$	-718.42	77.19	-4.81
(10)	$\text{C}_2\text{HCl}_2\text{OH}+\text{Cl}_2\rightarrow\text{HCl}+\text{CHCl}_2\text{COCl}$	-204.33	18.14	-165.74
(11)	$\text{CHCl}_2\text{COCl}+\text{CH}_3\text{COOH}\rightarrow\text{C}_4\text{H}_5\text{O}_3\text{Cl}_3$	-268.11	32.15	-55.43
(12)	$\text{C}_4\text{H}_5\text{O}_3\text{Cl}_3\rightarrow\text{CH}_3\text{COCl}+\text{CHCl}_2\text{COOH}$	-313.83	37.49	-105.67
(13)	$\text{CH}_3\text{COOH}+3\cdot\text{Cl}\rightarrow 3\cdot\text{H}+\text{CCl}_3\text{COOH}$	-170.98	192.12	153.60
(14)	$\text{CHCl}_2\text{COOH}+\cdot\text{Cl}\rightarrow\cdot\text{H}+\text{CCl}_3\text{COOH}$	-713.34	173.81	160.45
(15)	$\text{CHCl}_2\text{COCl}+\text{H}^+\rightarrow\text{H}^++\text{C}_2\text{Cl}_3\text{OH}$	-359.11	162.56	50.41
(16)	$\text{C}_2\text{Cl}_3\text{OH}+\text{Cl}_2\rightarrow\text{HCl}+\text{CCl}_3\text{COCl}$	-669.80	49.60	-127.90
(17)	$\text{CCl}_3\text{COCl}+\text{CH}_3\text{COOH}\rightarrow\text{C}_4\text{H}_4\text{O}_3\text{Cl}_4$	-91.74	107.34	-55.66
(18)	$\text{C}_4\text{H}_5\text{O}_3\text{Cl}_3\rightarrow\text{CH}_3\text{COCl}+\text{CCl}_3\text{COOH}$	-88.68	110.23	47.79

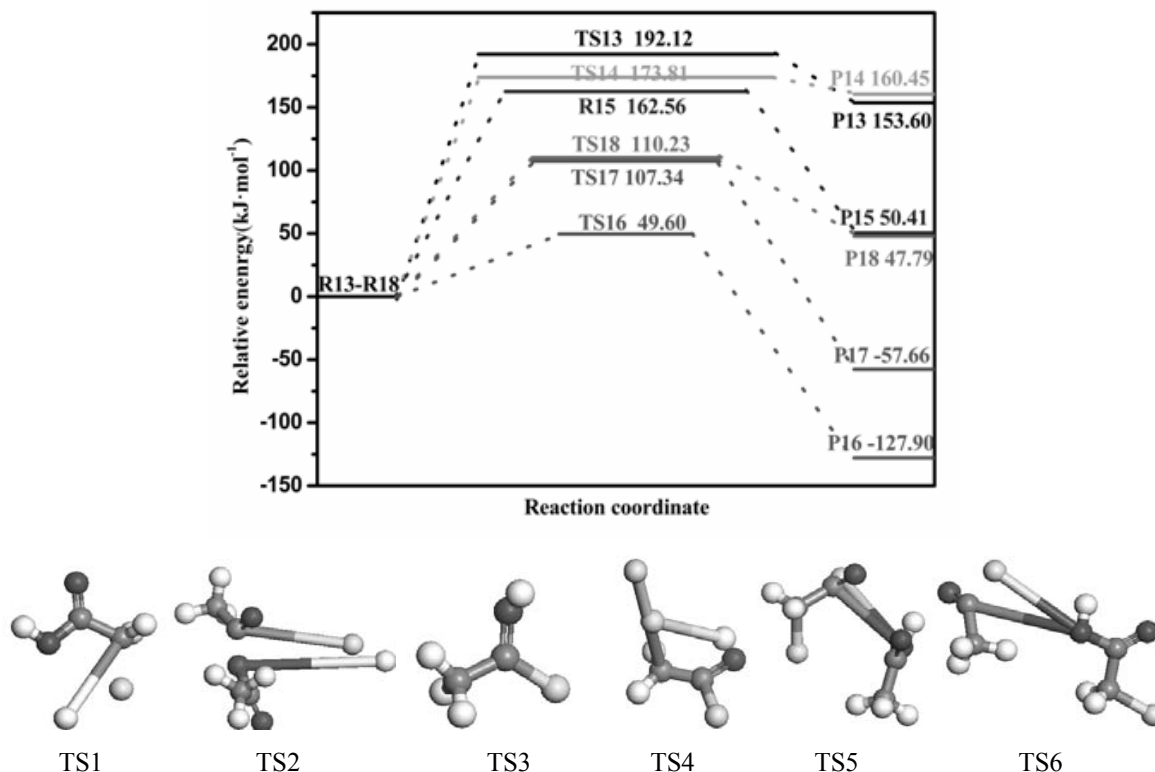


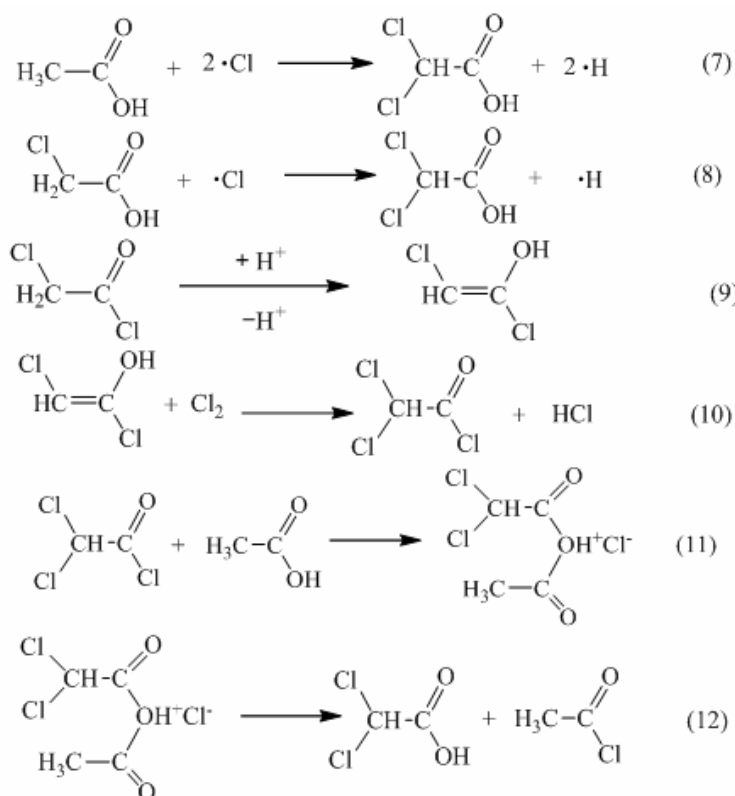
Fig. 3 – Potential energy diagram of monochloroacetic acid synthesis together with the initial states, transition states, and final states.

The activation energy 51.64 kJ/mol [Scheme 1, Equation (3)] was the highest as the rate-determining step after acetyl chloride was formed. Experimental results also showed that the formation rate of monochloroacetic acid was slow at the beginning and then became rapid in the mid of reaction after the addition of acetic anhydride catalyst. The reason of it could be that the process of acetic acid enolization was slow so that the production of 1-chloro, 1-ethene-1-ol was less, while with the increase of 1-chloro, 1-ethene-1-ol, the formation rate of monochloroacetic acid was also accelerated. Moreover, the contents of acetic acid which react with chloroacetyl chloride also reduced at the end of the reaction. Meanwhile, the rate of acid-catalysis enolization [Scheme 1, Equation (3)] was accelerated due to the fact that the acidity of monochloroacetic acid was stronger than of the acetic acid. Thus the generation speed of monochloroacetic acid was accelerated. In addition, the generation of monochloroacetic acid increased significantly when the concentrated H_2SO_4 and FeCl_3 were added. The added H^+ in the reaction system promoted the progress of acid-catalysis enolization [Scheme 1, Equation (3)]. In turn, it led to the result that the reaction was conducted towards the generation of monochloroacetic acid.

Therefore, it can be drawn from the theoretical calculation and experimental results that the whole process became acid catalytic enolization reaction when acetyl chloride was formed. The generation of monochloroacetic acid could be accelerated as long as acetyl chloride acid-catalyzed enolization [Scheme 1, Equation (3)] was expected. It also inhibited the generation of the byproduct dichloroacetic acid and trichloroacetic acid.

Synthesis chlorination mechanism of the byproduct dichloroacetic acid

In order to investigate the formation route of byproduct dichloroacetic acid, two possible reaction paths were constructed: the equilibrium reaction path and the consecutive reaction path (Scheme 2). The path 1 was the formation of dichloroacetic acid *via* equilibrium reaction route [Scheme 2, Equation (7)]. The path 2 was the formation of dichloroacetic acid *via* consecutive reaction route [Scheme 2, Equation (8)-(12)]. Moreover, there were two reaction mechanisms in the consecutive path: the radical chlorination mechanism and ionic chlorination mechanism.



Scheme 2 – The chlorination mechanism of byproduct dichloroacetic.

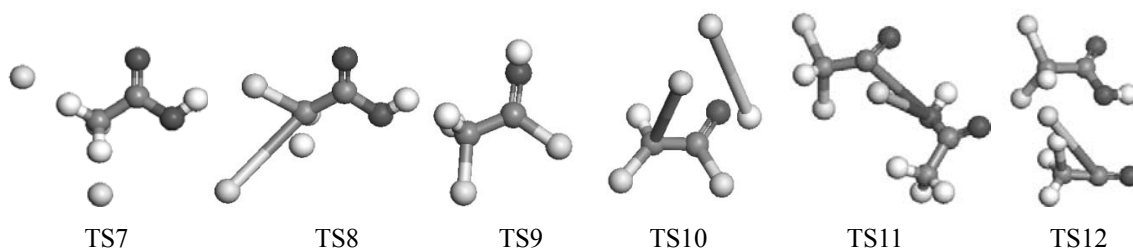
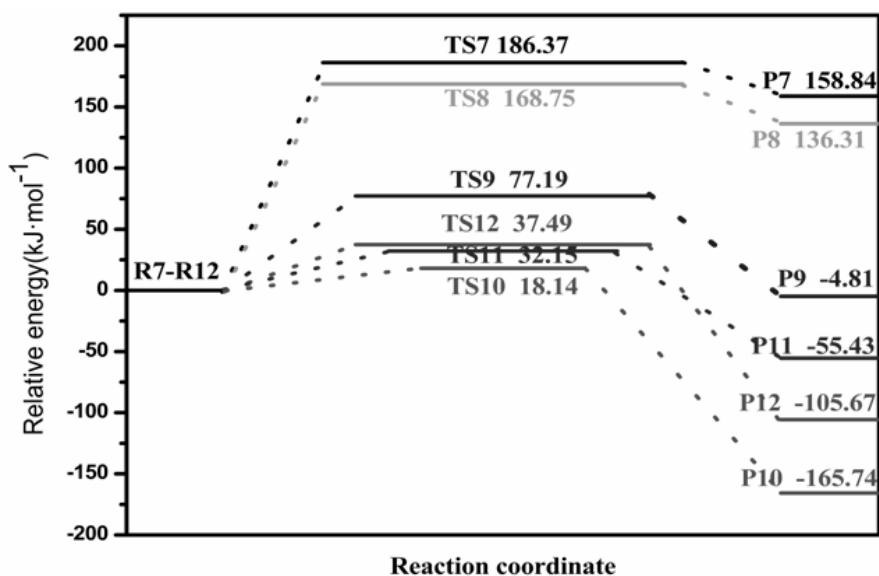


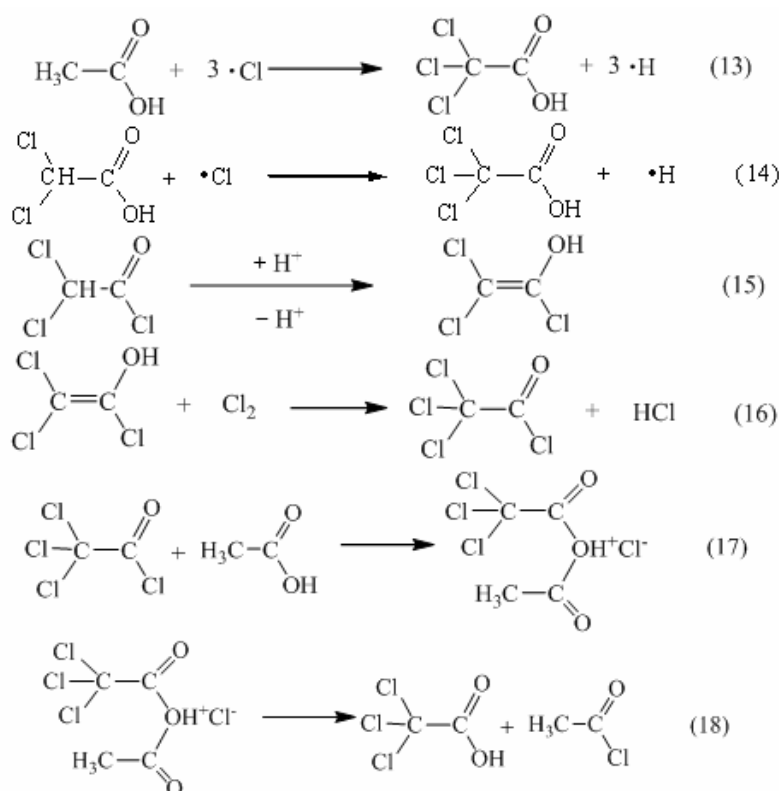
Fig. 4 – Potential energy diagram of byproduct dichloroacetic acid Synthesis together with the initial states, transition states, and final states.

As shown in Figure 4, the activation energy of radical equilibrium reaction that generated dichloroacetic acid [Scheme 2, Equation (7)] was 186.37kJ/mol, and the activation energy of generating dichloroacetic acid *via* radical consecutive reaction was 168.75 kJ/mol. [Scheme 2, Equation (8)] . In addition, the formation route of dichloroacetic acid *via* ionic chlorination mechanism was as follows: first, the chloroacetic chloride conducted enolization [Scheme 2, Equation (9)] and formed 1,2-dichloro, 1-ethene-1-ol and the corresponding primitive activation energy was 77.19kJ/mol. Then, the double bond in 1, 2-dichloro, 1-ethene-1-ol was apt to react with chloride [Scheme 2, Equation (10)] and formed 2, 2-dichloroacetyl chloride and the corresponding primitive activation energy was 18.14kJ/mol. Finally, the -OH and -Cl exchange reaction generated dichloroacetic acid [Scheme 2, Equation (11)-(12)] and their activation energy were 32.15kJ/mol and 37.49 kJ/mol, respectively. Compared to the two paths the activation energies formed dichloroacetic acid *via* radical chlorination mechanism [Scheme 2, Equation (8)] was higher than that formed the dichloroacetic acid *via* ionic chlorination mechanism [Scheme 2, Equation (9)-(12)]. Therefore, the formation route of dichloroacetic acid was mainly *via* ionic chlorination mechanism, and belonged to the ionic consecutive reaction route.

Chlorination mechanism of byproduct trichloroacetic acid

The formation mechanism of byproduct trichloroacetic acid was investigated based on the reaction mechanism of dichloroacetic acid. Two possible reaction paths were also constructed: the equilibrium reaction path and the consecutive reaction path (Scheme 3). The path 1 was the formation of trichloroacetic acid *via* equilibrium reaction route, which belonged to the radical chlorination mechanism [Scheme 3, Equation (13)]. The path 2 was the formation of trichloroacetic acid *via* consecutive reaction route, which included the radical chlorination mechanism and ionic chlorination mechanism [Scheme 3, Equation (14)

(18)]. In path 2, the dichloroacetyl chloride conducted acid-catalysis enolization [Scheme 3, Equation (15)] and formed 2,2-dichloro, 1-vinyl alcohol. The consecutive chlorination of 2,2-dichloro, 1-vinyl alcohol with chlorine generated trichloroacetyl chloride [Scheme 3, Equation (16)]. Finally, trichloroacetyl chloride with acetic acid generated trichloroacetic acid by the -OH and -Cl exchange reaction [Scheme 3, Equation (17)-(18)]. At the same time, the potential energy diagram of the primitive reaction, the corresponding reactions, transition states and products of configuration were shown in Figure 5.



Scheme 3 – The chlorination mechanism of byproduct trichloroacetic acid.

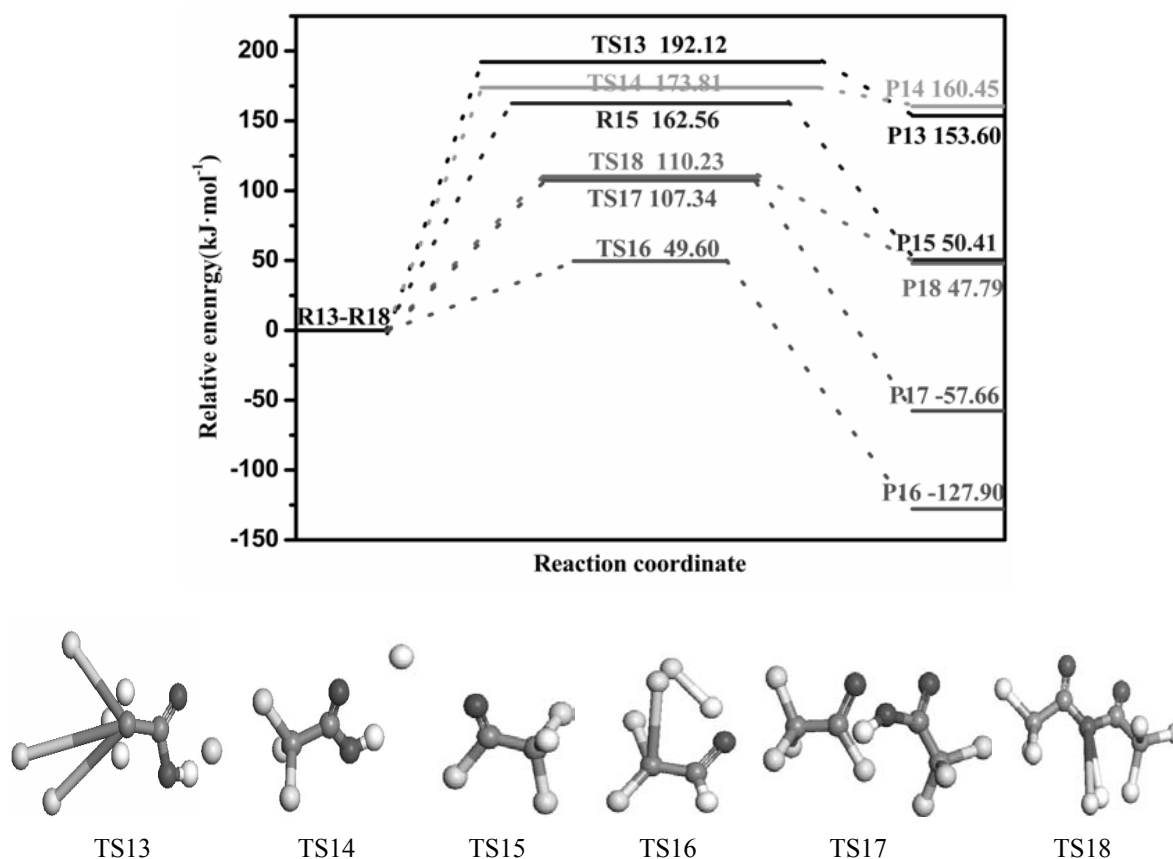


Fig. 5 – Potential energy diagram of byproduct trichloroacetic acid Synthesis together with the initial states, transition states, and final states.

As shown in Figure 5, the activation energy of radical equilibrium reaction was 192.12 kJ/mol [Scheme 3, Equation (13)], which was higher than the activation energy of radical consecutive reaction as 173.81 kJ/mol. [Scheme 3, Equation (14)]. Moreover, the activation energy of the process of trichloroacetic acid chlorination *via* ionic chlorination mechanism was the highest as 162.56 kJ/mol [Scheme 3, Equation (15)], which was the rate-determining step. Further comparison showed that the radical chlorination activation energy 173.81 kJ/mol [Scheme 3, Equation (14)] was higher than 162.56 kJ/mol [Scheme 3, Equation (15)]. It implied that the radical chlorination was not easy to occur as ionic chlorination. Thus, the formation route of trichloroacetic acid was mainly through ionic chlorination mechanism, and belonged to the ionic consecutive reaction.

Moreover, comparing to the activation energy of the byproduct dichloroacetic acid and trichloroacetic acid in the generation path, it could be found that the activation energy of the trichloroacetic acid rate-determining step 162.56 kJ/mol [Scheme 3, Equation (15)] was

higher than 77.19 kJ/mol [Scheme 2, Equation (9)]. Therefore, dichloroacetic acid was the main byproduct, trichloroacetic acid was minor byproduct. The generation of trichloroacetic acid *via* dichloroacetyl chloride, in result of inhibiting the generation of dichloroacetic acid could effectively decrease the production of trichloroacetic acid.

CONCLUSION

The article investigated the chlorination mechanism from acetic acid to monochloroacetic acid. The results were as follows:

The activation energy of ionic mechanism for monochloroacetic acid was lower than that of radical mechanism. The generation process of 1-chloro,1-ethene-1-ol *via* chloroacetyl chloride acid-catalyzed enolization was the rate determining step in the ionic reaction path.

It was observed that in this experiment the formation rate of monochloroacetic acid was slow at the beginning and became rapid in the mid, then slowed down again in the latter. The generation

rate of acetyl chloride enolization was slow at the beginning, then increased with the increase of monochloroacetic acid. The reason was that the acidity of monochloroacetic acid was stronger than of acetic acid, which made the acid catalysis become as an acid catalyzed autocatalytic process.

The generation of monochloroacetic acid increased rapidly when the concentrated H_2SO_4 and FeCl_3 catalyst were added. It was observed that H^+ promoted the process of acid-catalysis enolization. In turn, it led to the result that the reaction was conducted towards the generation of monochloroacetic acid.

The formation path of byproduct dichloroacetic acid and trichloroacetic acid was mainly through ionic consecutive chlorination mechanism.

Acknowledgements. All calculations in this paper were accomplished in the Key Laboratory of Coal Science and Technology, Ministry of Education and Shanxi Province. The authors are indebted to Prof. Wang Baojun and Prof. Zhang Riguang because of their strong support.

REFERENCE

1. Y. L. Mu and X. A. Wang, *China Chlor-Alkali.*, **2008**, *12*, 12–14.
2. J. Herold, “Ueber die Reaktionskinetik der katalytischen Chlorierung von Essigsäure”, Diss. Nr. 4141, Eidgenössische Technische Hochschule, Zurich, **1968**.
3. P. Martikainen, T. Salmi, E. Paatero and L. Hummelstedt, *J. Chem. Technol. Biotechnol.*, **1987**, *40*, 259–274.
4. G. Sioli, P. Spaziante and L. Giuffrè, *Hydrocarbon Process.*, **1979**, *2*, 111.
5. Y. Ogata, T. Sugimoto and M. Inaishi, *Bull. Chem. Soc. Jpn.*, **1979**, *52*, 255–256.
6. Y. Ogata, K. Harada, K. Matsuyama and T. Ikejiri, *J. Org. Chem.*, **1975**, *40*, 2960–2962.
7. T. Salmi, P. Martikainen, E. Paatero, L. Hummelstedt, H. Damen and T. Lindroos, *Chem. Eng. Sci.*, **1988**, *43*, 1143.
8. P. Mäki-Arvela and T. Salmi, *Ind. Eng. Chem. Res.*, **1994**, *33*, 2073–2083.
9. X. Y. Zhou, *J. Wuhan Uni. Sci. Tech. (China)*, **2006**, *29*, 161–175.
10. P. Mäki-Arvela, T. Salmi and E. Paatero, *Chem. Eng. Sci.*, **1995**, *50*, 2275–2288.
11. C. J. Xia, L. Ju, Y. Zhao, H. Y. Xu, B. Zhu, F. F. Gao, M. Lin, Z. Y. Dai, X. D. Zou and X. T. Shu, *Chinese. J. Catal.*, **2015**, *36*, 845–852.